Skeletal parasympathetic innervation communicates central IL-1 signals regulating bone mass accrual

Alon Bajayo[a], Arik Bar[a], Adam Denes[b,c], Marilyn Bachar[a], Vardit Kram[a], Malka Attar-Namdar[a], Alberta Zallone[d], Krisztina J. Kovács[c], Raz Yirmiya[e], and Itai Bab[a,1]

[a]Bone Laboratory and [e]Department of Psychology, Hebrew University of Jerusalem, Jerusalem 91120, Israel; [b]Faculty of Life Sciences, University of Manchester, Manchester M13 9PT, United Kingdom; [c]Laboratory of Molecular Neuroendocrinology, Institute of Experimental Medicine, Budapest H-1450, Hungary; and [d]Department of Human Anatomy and Histology, University of Bari, Bari 70124, Italy

Bone mass accrual is a major determinant of skeletal mass, governed by bone remodeling, which consists of bone resorption by osteoclasts and bone formation by osteoblasts. Bone mass accrual is inhibited by sympathetic signaling centrally regulated through activation of receptors for serotonin, leptin, and ACh. However, skeletal activity of the parasympathetic nervous system (PSNS) has not been reported at the bone level. Here we report skeletal immune-positive fibers for the PSNS marker vesicular ACh transporter (VAChT). Pseudorabies virus inoculated into the distal femoral metaphysis is identifiable in the sacral intermediolateral cell column and central autonomic nucleus, demonstrating PSNS femoral innervation originating in the spinal cord. The PSNS neurotransmitter ACh targets nicotinic (nAChRs), but not muscarinic receptors in bone cells, affecting mainly osteoclasts. nAChR agonists up-regulate osteoclast apoptosis and restrain bone resorption. Mice deficient of the α_2nAChR subunit have increased bone resorption and low bone mass. Silencing of the IL-1 receptor signaling in the central nervous system by brain-specific overexpression of the human IL-1 receptor antagonist ($hIL1ra_{Ast}^{+/+}$ mice) leads to very low skeletal VAChT expression and ACh levels. These mice also exhibit increased bone resorption and low bone mass. In WT but not in $hIL1ra_{Ast}^{+/+}$ mice, the cholinergic ACh esterase inhibitor pyridostigmine increases ACh levels and bone mass apparently by inhibiting bone resorption. Taken together, these results identify a previously unexplored key central IL-1–parasympathetic–bone axis that antagonizes the skeletal sympathetic tone, thus potently favoring bone mass accrual.

autonomic nervous system | postnatal skeletal development

I n vertebrates, bone mass is the major factor affecting skeletal strength. Bone mass is determined by a continuous remodeling process consisting of bone resorption by osteoclasts and bone formation by osteoblasts. Skeletal remodeling during bone mass accrual in early life favors bone formation. Age-related bone loss results from a net increase in bone resorption (1). Bone mass is regulated by an intricate system including central cues, so far shown to be transmitted mainly via the sympathetic nervous system (SNS), which tonically restrains bone formation and stimulates bone resorption, thus downregulating bone mass accrual (2, 3). Increased sympathetic output mediates low bone mass in depression (4), whereas decreased skeletal sympathetic signaling mediates traumatic brain injury-induced increase in bone formation (5).

In most biological systems (e.g., heart, eye pupil, digestive track, glucose metabolism, and exocrine glands) the SNS is antagonized or complemented by the parasympathetic nervous system (PSNS) (6–10). These two arms of the autonomic nervous system traverse distinct anatomical routes. Preganglionic cells of the SNS extend from the first thoracic spinal segment to the third lumbar segment. The cell bodies of these neurons are found within the spinal cord, primarily within the intermediolateral gray matter (11). The preganglionic neurons of the PSNS that innervate the rostral part of the body project parasympathetic

cranial nerves originating from the brainstem. Sacral preganglionic neurons, which innervate the caudal part of the body, occupy the central autonomic nuclei and the sacral extention of the intermediolateral column (11).

The main neurotransmitter in use by the SNS is norepinephrine, whereas that of the PSNS is ACh, the first identified neurotransmitter (12). ACh is biosynthesized in presynaptic neurons by acetylation of choline, a process catalyzed by choline acetyltransferase (13). For release into the synaptic space, ACh is packaged in presynaptic vesicles through the action of another enzyme, vesicular ACh transporter (VAChT). The concentration of VAChT increases progressively with proximity to the nerve terminals: it is thus considered a hallmark and a selective marker of parasympathetic innervation (14, 15). ACh targets nicotinic ACh receptors (nAChR), which are homopentamers consisting of α-subunits and heteropentamers comprised of α-, β-, γ-, δ-, and ε-subunits. nAChR function primarily as ion channels (16). In addition, ACh binds to and activates seven transmembrane domain muscarinic receptors (17). Another critical component of the PSNS is ACh esterase (AChE), which is expressed by postsynaptic cells and degrades ACh, thus limiting its action (18).

It has been shown in the central nervous system that the skeletal SNS activity is down-regulated through the activation of muscarinic receptors (19). In addition, expression of receptors for ACh have been reported in bone cells (20), which raises the prospect that the PSNS antagonizes or complements sympathetic activity at the bone level.

In health, central IL-1 signaling has been implicated in modulating sleep patterns (21), learning, and memory (22). Previously, we showed that central nervous system-targeted silencing of the IL-1 receptor by brain-specific overexpression of the human IL-1 receptor antagonist ($hIL1ra_{Ast}^{+/+}$ mice) inhibits bone mass accrual (23). Because this activity mirrors the SNS skeletal activity, we reasoned that the PSNS communicates central IL-1 cues to the skeleton. Indeed, we show here that bone is innervated by the PSNS, leading to a positive tone, which up-regulates bone mass accrual. We further demonstrate that PSNS outputs are critically regulated by central IL-1 signaling.

Results

Skeletal Parasympathetic Innervation. Because PSNS regulation has not been previously demonstrated at the bone level, we first sought to characterize the cholinergic pathway innervating the skeleton. Indeed, immunohistochemical staining of trabecular

MEDICAL SCIENCES

bone in the distal femoral metaphysis demonstrated VAChT-positive neuronal fibers (Fig. 1 *A* and *B*) in medullary intertrabecular spaces, mainly in the close vicinity of bony struts, one-to-three cell layers away from their surface (Fig. 1 *A* and *B*, and Fig. S1*A*). To map the central autonomic pathway controlling these neurons, retrograde transneuronal tracing was carried out using a recombinant pseudorabies virus inoculated into the distal femoral metaphysis (24) (Fig. S1*B*). Virus-labeled cell bodies were identified in the intermediolateral column and central autonomic nucleus of the sacral spinal cord segment of mice and rats (Fig. 1*C* and Fig. S1*C*), anatomical sites restricted for parasympathetic preganglionic cell bodies. Consistent with SNS innervation of the femur (24), the intermediolateral column was also labeled at the thoracic level (Fig. S1*D*), known to harbor sympathetic preganglionic cells (11). The central autonomic nucleus was also labeled at this level (Fig. S1*D*), a finding previously attributed to interneuronal pseudorabies virus infection (25, 26). That other skeletal sites, and possibly the entire skeleton, are functionally innervated by the PSNS is suggested by the low bone mass found in lumbar vertebral bodies of young adult mice after subdiaphragmatic vagotomy (27) (Fig. S1*E*).

Bone Cell Expression of Receptors for ACh. To elucidate the receptors for ACh expressed in bone cells, we screened RNA from osteoblasts, monocytes, and osteoclasts for the expression of all muscarinic receptors and nAChR subunits. Muscarinic receptors are not detectable with conventional RT-PCR. Several mRNA transcripts for neuronal and muscular type nAChR subunits are present in osteoclasts and osteoblasts (Fig. 2*A*). The most abundantly expressed subunit in osteoclasts is α_2nAChR; notably, it is also expressed, although at a lower level, in monocytic osteoclast precursors (Fig. 2*A*). At the protein level, osteoclastic expression of the α_2nAChR subunit is clearly detectable in osteoclasts in ex vivo cultures (Fig. 2*B*) and in vivo in bone histological sections (Fig. 2*C*). The β_2nAChR subunit is also highly expressed in osteoclasts (Fig. 2 *A* and *D*) as well as in osteoblasts (Fig. 2 *A* and *E*). The high affinity $\alpha_2\beta_2$nAChR subtype has been reported in the central nervous system and retina (28), and the present expression analysis suggests that it is the main subtype functional in osteoclasts.

Low Bone Mass in α_2nAChR-Deficient Mice. Because the α_2- and β_2nAChR subunits can form receptor complexes (28), and because α-subunits are essential components of nAChRs, we analyzed the skeletal phenotype of α_2nAChR$^{-/-}$ mice (29). These mice show a marked low bone mass (Fig. 3*A* and Table S1), mainly because of a vast increase in bone resorption reflected by approximately twofold increases in the number of tartrate-resistant acid phosphatase- (TRAP) positive osteoclasts (Fig. 3*B*) and serum C-telopeptide of type I collagen level (Fig. 3*C*). The α_2nAChR gene deletion had no significant effect on bone formation (Fig. S2). These findings suggest that nAChRs that include the α_2nAChRs subunit have a key role in regulating skeletal remodeling mainly through an inhibitory tone of bone resorption.

Cholinergic Signaling Inhibits Bone Resorption by Stimulating Osteoclast Apoptosis. To elucidate the mechanism mediating the PSNS inhibition of osteoclast number we assessed the effect of the AChE-resistant cholinergic agonists carbamylcholine (CCh) and nicotine on osteoclast formation, survival, and activity in ex vivo bone marrow-derived osteoclastogenic cultures. Cholinergic activation has no effect on the overall number of or size of the osteoclasts (Fig. S3 *A* and *B*). However, both agonists induce a marked, dose-dependent decrease in the number of intact WT but not α_2nAChR$^{-/-}$ TRAP-positive osetoclasts (Fig. 4 *A* and *B*, and Fig. S3 *C* and *E*), confirming that α_2nAChR expression is critical for the cholinergic regulation of bone resorption at the PSNS target-cell level rather than elsewhere upstream the PSNS–bone axis. The agonist-induced reduction in the number of intact WT osteoclasts is accompanied by an ~10-fold increase in the number apoptotic osteoclasts (Fig. 4 *C* and *D*, and Fig. S3*D*). This agonist effect is inhibited by the nAChR antagonist mecamylamine (30) (Fig. 4*E*). Expectedly, cholinergic agonist treatment does not affect the number of α_2nAChR$^{-/-}$ apoptotic osteoclasts (Fig. S3*E*). Consistent with the decrease in osteoclast number and increase in apopototic-like osteoclasts, CCh induces a marked decrease in mRNA levels of the osteoclast marker gene *Trap5b* (Fig. 4*F*) as well as in the mRNA expression of the antiapoptotic gene *Bcl2L1* (Fig. 4*G*). In line with the increase in apoptotic-like osteoclast number and decrease in *Bcl2L1* expression, osteoclastic caspase 3 activity is increased by almost threefold by the CCh treatment (Fig. 4*J*). Expression of the proapoptotic gene Bid and the extracellular matrix degrading enzyme cathepsin K are unaffected by CCh (Fig. 4 *H* and *I*). These findings suggest that PSNS cholinergic signaling specifically stimulates osteoclast apoptosis. To assess the impact of increased osetoclast apoptosis on bone resorption we tested the effect of CCh on pit excavation in dentin slices, an ex vivo surrogate for the breakdown of mineralized matrices (31). CCh has no effect on the number of pits (Fig. 4*K*), confirming that cholinergic activity does not affect osteoclastogenesis. However, CCh induces nearly 50% reduction in pit area (Fig. 4 *L* and *M*), suggesting that nAChR activation shortens the duration of osteoclast activity, which in turn results in reduced bone resorption.

nAChR Agonists Regulate Osteoblast Proliferation. Osteoblasts express mainly the muscular type α1-, β1-, and γ-subunits, as well as the neuronal subunits α4, α7, β2, and β4 (Fig. 2 *A* and *E*). As in the case of other fibroblast-like cells (32), CCh and nicotine have a biphasic effect on osetoblast proliferation, consisting of a dose-response stimulation of cell number peaking at 10^{-10} M agonist concentration, followed by reversal of this stimulation at higher concentrations (Fig. S4*A*), presumably because of nAChR desensitization. The stimulation is equally inhibitable by the nonspecific cholinergic antagonist mecamylamine (30) (Fig. S4*B*) and the muscle-type–specific nAChR antagonist tubocurarine (33) (Fig. S4*C*), portraying the muscle-type nAChR as the prevailing cholinergic receptor in osteoblasts. Expression of the osteoblastic genes encoding for osterix, alkaline phosphatase, osteocalcin, osteoprotegerin, and receptor activator of NFκB ligand (RANKL) is unaffected by cholinergic stimulation (Fig. S4*D*), suggesting that cholinergic agonists regulate the
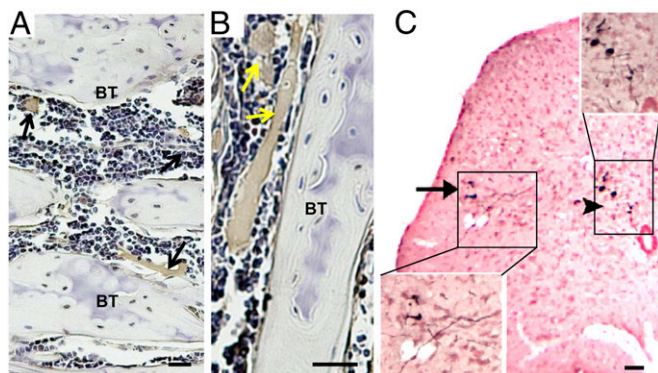

Fig. 1. Parasympathetic innervation in bone. (*A* and *B*) VAChT-positive nerve fibers (arrows) in distal femoral metaphysis. BT, bone trabeculae. (*A*) Low- and (*B*) high-power view. (*C*) Propagation of immunoreactive pseudorabies virus from distal femoral metaphysis to sacral spinal cord segments of intermediolateral column (arrow) and central autonomic nucleus (arrowhead). (*Insets*) Higher magnification of boxed zones. (Scale bars, 50 μm.)
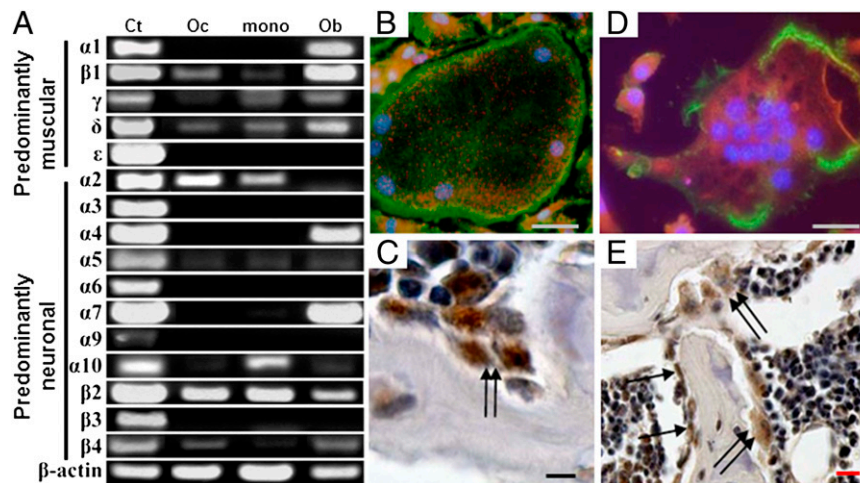
Fig. 2. Expression of nicotinic receptors in bone cells. (*A*) RT-PCR analysis of nicotinic receptor subunits in primary cultures of newborn mouse calvarial osteoblasts (Ob) bone marrow-derived monocytes (mono) and osteoclasts (Oc). Ct, positive control of whole brain or skeletal muscle RNA extract. (*B–E*) Immunocytochemical staining for nicotinic receptor subunits in osteoclasts and osetoblasts. (*B* and *D*) Osteoclasts in culture; red, subunit (*B*) α_2-subunit, (*D*) β_2-subunit; green, actin; blue, nuclei. (*C* and *E*) in-vivo immunohistochemistry of femoral trabecular bone; arrows, osteoblasts; double arrows, osteoclasts: (*C*) α_2-subunit, (*E*) β_2-subunit. (Scale bars, 20 μm.)

number of osteoblasts rather than their differentiation or activity. The absence of changes in osteoprotegerin and RANKL mRNA levels further suggests that the effect of cholinergic agonists on osteoclasts is cell autonomous and not mediated by osteoblasts.

PSNS Regulation by Central IL-1 Signaling. We have previously reported that although peripheral IL-1 is pro-osteoclastic, central IL-1 signaling increases bone mass by suppressing bone resorption, as $hIL1ra_{Ast}^{+/+}$ mice have a low bone mass phenotype, secondary to increased osteoclastic activity (23). We confirm now

Fig. 3. Low bone mass phenotype in $\alpha_2nAChR^{-/-}$ mice. (*A*) Bone volume density (BV/TV) and 3D μCT images from representative animals with median BV/TV values; (*B* and *C*) Bone remodeling parameters in distal femoral metaphysic: (*B*) osteoclast number (scale bar, 20 μm); (*C*) serum C-telopeptide of type I collagen (CTX). Data are mean ± SE obtained in six to nine mice per condition. *t test, $P < 0.05$ vs. WT controls.

that this phenotype is restricted to bone mass accrual (Fig. S5) and is reminiscent of the low bone mass observed in $\alpha_2nAChR^{-/-}$ mice (Fig. 3) and following vagotomy in WT animals (Fig. S1*E*). Therefore, we tested whether $hIL1ra_{Ast}^{+/+}$ mice have altered parasympathetic activity. Indeed, following β-adrenergic blockage by propranolol, which unmasks the parasympathetic cardiac contribution, the heart rate drop in these mice is significantly smaller than in WT controls (Fig. 5*A*). In addition, skeletal VAChT expression is almost completely arrested in the trabecular bone of $hIL1ra_{Ast}^{+/+}$ mice (Fig. 5*B*). This vast decrease in VAChT expression is apparently part of a generalized dysregulation of the PSNS, which leads to a marked decrease in bone ACh levels (Fig. 5*C*). Taken together, these findings suggest that central IL-1 signaling, at least at physiological levels, is involved in regulating the PSNS. AChE, the ACh-degrading enzyme, is expressed in bone cells (Fig. S6*A*). Thus, to further evaluate and establish the skeletal impact of the central IL-1–PSNS–bone axis, we tested the effect of pyridostigmine, a peripheralized AChE inhibitor (34), on the skeletocholinergic phenotype of WT and $hIL1ra_{Ast}^{+/+}$ mice during bone mass accrual. At the dosing protocol used (1 mg·kg·d) pyridostigmine does not cause nAChR desensitization because of sustained exposure to increased ligand concentration (35). Expectedly, daily pyridostigmine administration between the ages of 5 and 11 wk stimulates bone ACh levels in WT but not in $hIL1ra_{Ast}^{+/+}$ mice (Fig. 5*C*), confirming that impaired parasympathetic activity in bone is tightly linked to reduced central IL-1 signaling. In line with these data and the postvagotomy low bone mass (Fig. S1*E*), pyridostigmine stimulated trabecular bone mass in WT animals but not in $hIL1ra_{Ast}^{+/+}$ mice (Fig. 5*D* and Table S2). The low bone mass in $hIL1ra_{Ast}^{+/+}$ mice is secondary to more than doubling the number of TRAP-positive osteoclasts, with only a minor effect on bone formation, if any (Fig. 5 *E* and *F*). As in the case of bone mass, pyridostigmine affected the number of TRAP-positive osteoclasts only in WT mice (Fig. 5*E*). Like central IL-1 receptor silencing, pyridostigmine has no effect on bone formation (Fig. 5*F*). In view of the biphasic ex vivo effect of nAChR agonists on osteoblast number and the difference between optimal agonist concentration in the osteoclast and osteoblast cultures (compare Fig. 4*A* and Fig. S4*A*), these data suggest that the bone ACh concentration is optimal for restraining osteoclast number but supraoptimal for the stimulation of bone formation.
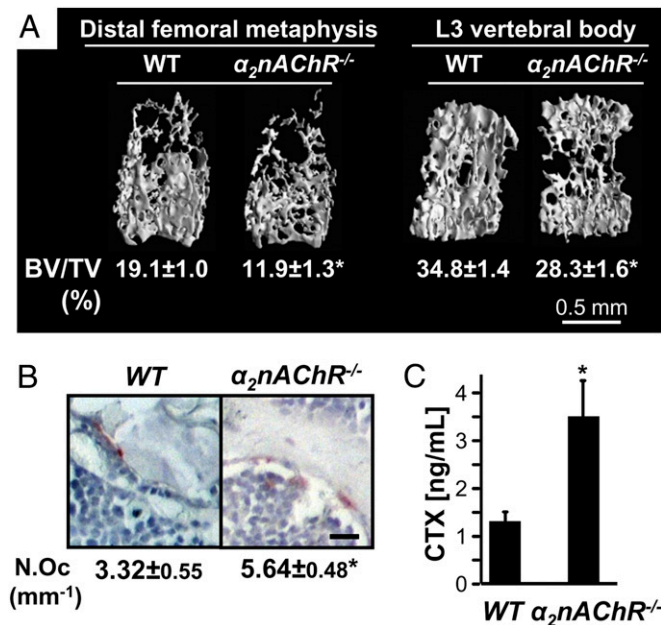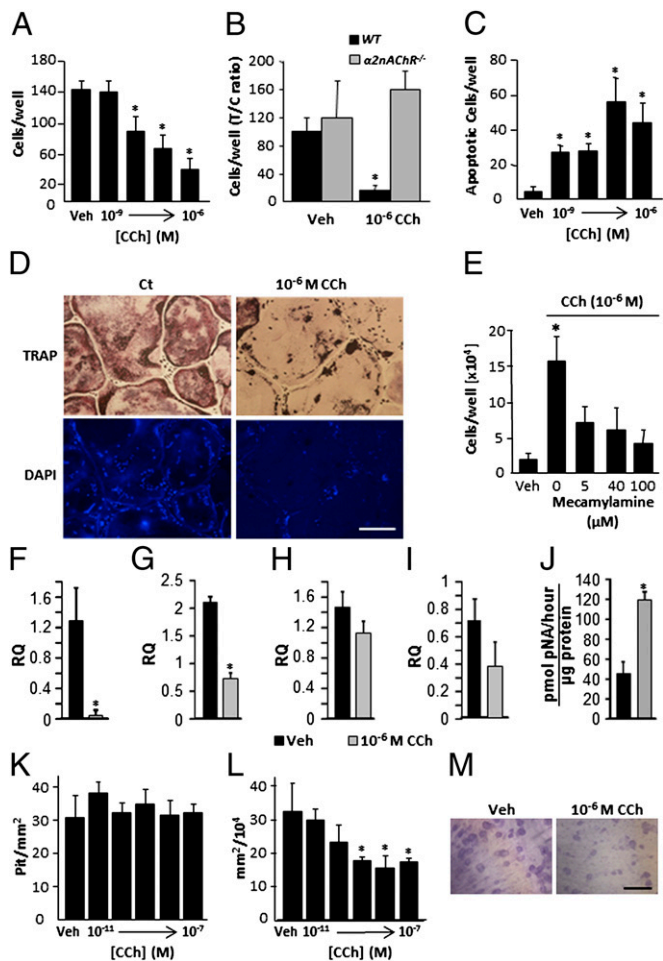
Fig. 4. nAChR activation enhances osteoclast apoptosis and inhibits mineralized matrix resorption. (A–J) Effect of CCh in bone marrow derived osteoclastogenic cultures. (A and B) Intact osteoclasts derived from WT (black bars) and $\alpha_2 nAChR^{-/-}$ (gray bars) mice. (C) WT apoptotic osteoclasts. (D) In situ images of intact and apoptotic osteoclasts in respective control and CCh-treated cultures. (Scale bar, 500 μm.) (E) Apoptotic osteoclasts treated with CCh and mecamylamine. (F–I) Real-time RT-PCR analysis of osteoclastic genes in intact osteoclasts. (F) Trap5b; (G) Bcl2L1; (H) Bid; (I) Cathepsin K; (J) caspase 3 activity. pNA, p-nitroaniline. (K–M) Pit formation in osteoclastogenic cultures of intact cells grown on dentin slices. (K) Pit number, (L) average pit size, (M) toluidine blue staining of vehicle and CCh treated dentin slices. (Scale bar, 100 μm.) Data are mean ± SE obtained in five to six (A–E, K, and L) or three (F–J) culture wells per condition. *$P < 0.05$, vs. WT vehicle-treated controls (Veh). (A, C, E, K, and L) one-way ANOVA; (B) two-way ANOVA; (F–J) t test.

Discussion

This study uncovers skeletal innervation by the PSNS consisting of functional cholinergic nerve fibers, production of the PSNS neurotransmitter ACh, as well as bone cell expression of ACh receptors and its rate-limiting enzyme, AChE. We provide further evidence for a previously unexplored regulation of the PSNS by central IL-1 signaling.

That this IL-1–PSNS–bone axis involves the entire skeleton is suggested by the low bone mass in both axial (vertebrae) and appendicular (femora) skeletal parts of $hIL1ra_{Ast}^{+/+}$ mice and failure of pyridostigmine and ACh to induced high bone mass in these mice. As in the case of other caudal PSNS targets, such as the lower gastrointestinal tract and genitalia (11), the PSNS innervation to the femur originates in the spinal cord, as suggested by the retrograde tracing of pseudorabies virus from this bone to the sacral intermediolateral column and central autonomic

nucleus. The vagus is the cranial nerve that carries PSNS innervation to the rostral part of the trunk (11). Therefore, the low bone mass in the lumbar vertebrae following subdiaphragmatic vagotomy suggests that, like the heart and eye, PSNS innervation of the rostral part of the skeleton is via cranial nerves. Our findings in the heart further suggest that this regulation is rather generalized involving the skeleton as well as nonskeletal tissues and organs.

Although the SNS targets primarily osteoblasts (36), our previous findings in $hIL1ra_{Ast}^{+/+}$ mice (23) and the present data
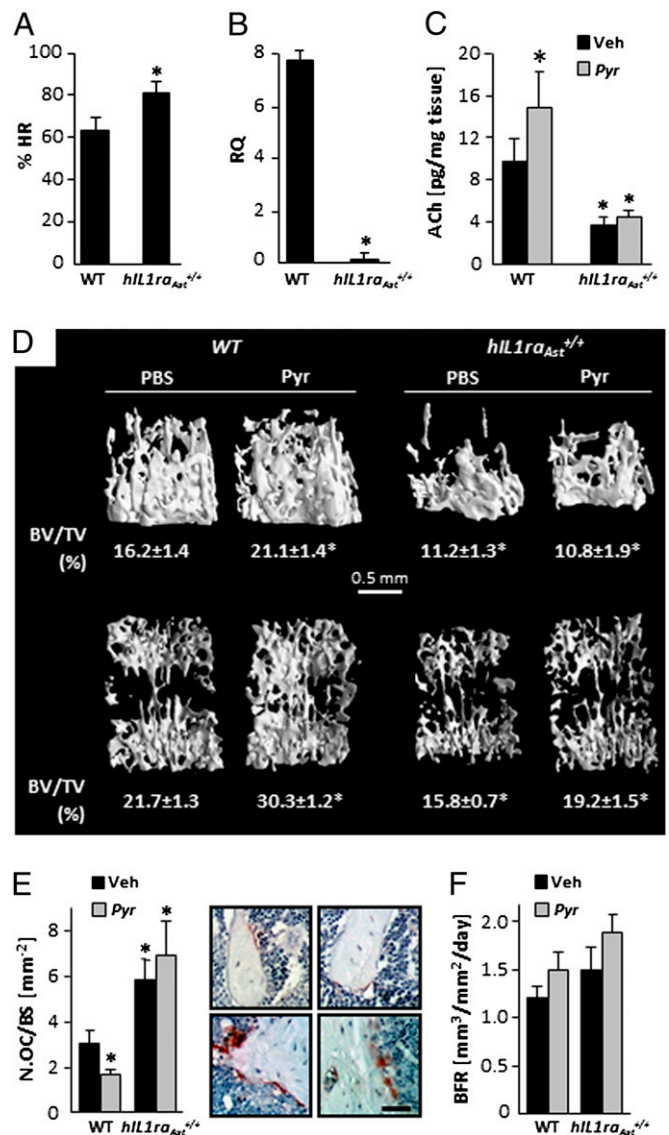

Fig. 5. Cardiac and skeletal parasympathetic signaling is regulated by central IL-1 receptor activity. (A–F) Reduced parasympathetic tone in $hIL1ra_{Ast}^{+/+}$ mice. (A) Percentage of pretreatment heart rate following propranolol administration; (B) VAChT mRNA levels in distal femoral metaphysis. (C–F) Cholinergic and bone remodeling parameters in vehicle and pyridostigmine-treated mice: (C) ACh levels in distal femoral metaphysis; (D) μCT representative images of distal femoral metaphyses (Upper), and L3 vertebral bodies (Lower) from animals with median volume density (BV/TV) values and actual BV/TV determination. (E and F) Analysis of bone resorption and bone formation in distal femoral metaphysis. (E) Osteoclast number (Oc.N/BS) and representative images of TRAP-stained sections from WT (Upper) and $hIL1ra_{Ast}^{+/+}$ (Lower) mice treated with vehicle (Left) or pyridostigmine (Right). (Scale bar, 80 μm.) (F) Bone formation rate (BFR). Data are mean ± SE obtained in 5–10 mice per condition. *$P < 0.05$ vs. WT vehicle treated controls. (A and B) t test; (C and F) two-way ANOVA.
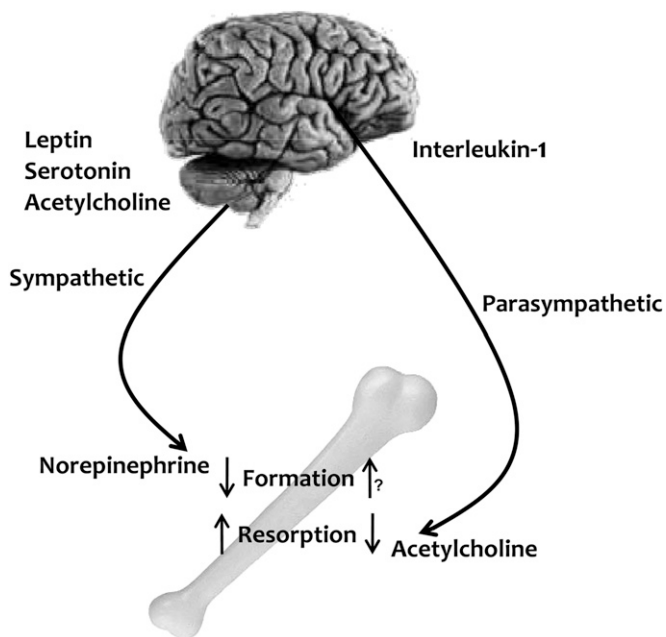
Bajayo et al.

Fig. 6. Model of autonomic regulation of bone mass accrual. Skeletal sympathetic tone, which inhibits bone formation and stimulates bone resorption, is centrally regulated by leptin, serotonin, and acetylcholine (19). It is antagonized by parasympathetic activity controlled by brain IL-1 signaling and results in enhanced bone formation and restrained bone resorption.

suggest that osteoclast apoptosis is the main process affected by the central IL-1–PSNS–bone axis. Although this and other reports show that osteoblasts express several nAChRs subunits (37), no significant changes in bone formation were found following central IL-1 receptor silencing or stimulation of skeletal ACh levels by pyridostigmine treatment. Although low concentrations of nAChRs agonists are mitogenic to osteoblasts, this effect is reversed by higher concentrations, shown to induce osteoclast apoptosis. It thus appears that physiologically ACh regulates only bone resorption and that the cholinergic regulation of osteoblast number becomes effective only when ACh levels are reduced in an attempt to attenuate the noradrenergic inhibition of bone formation (4) in situations such as stress, depression, and pain disorders (38).

The nAChR subunit profile demonstrated here in osteoblasts is reminiscent of previously reported expression profiles (37). Although muscarinic receptors have been recently described in human bone samples and in in vitro osteoblast models (39), we and others were unable to show significant levels of these receptors in bone cells and their conditional deletion in osteoblasts has no skeletal effects (19). In line with our mRNA and histochemical analyses, we show that deletion of the α_2nAChR subunit leads to a marked low bone mass during the developmental phase of the skeleton, because of a vast increase in osteoclast number and bone resorption. We also show that the main βnAChR subunit is β_2, thus portraying the $\alpha_2\beta_2$nAChR subtype as necessary for the cholinergic antiresorptive tone. Highly relevant to the central control of the PSNS is the close similarity between the $hIL1ra_{Ast}^{+/+}$ and $\alpha_2nAChR^{-/-}$ skeletal phenotypes.

ACh is released from PSNS nerve endings as well as from nonneuronal cells, thus functioning in an autocrine or paracrine manner (40). Indeed, VAChT and choline acetyltransferase mRNAs have been reported in murine osteoblasts (41). Therefore, ACh might act in an autocrine manner to enhance cell proliferation in bone. However, the protein level of at least VAChT is probably very low in nonneuronal bone and bone

marrow cells compared with its level in PSNS neurons inasmuch as our immunohistochemical staining for VAChT failed to show positive cells other than neurons. In addition, the central IL-1 receptor silencing resulted in almost complete absence of skeletal VAChT mRNA expression and a marked reduction in bone ACh levels, stressing the predominance of neuronal-derived ACh.

The present findings add important components to the model of central control of bone mass via the autonomic nervous system (Fig. 6). Low bone mass and osteoporosis are common comorbidities of neuropsychiatric disorders, such as depression, Alzheimer's disease, and epilepsy, which exhibit dysregulated autonomic activity, including changes in the PSNS (42–45). The present results, together with these observations and the central muscarinic stimulation of bone formation through down-regulation of the skeletal adrenergic tone (19), suggest that the PSNS is a master regulator of bone mass. Moreover, our findings may have broader implications, as the identified IL-1–PSNS axis likely also controls the immune system, inasmuch as both central IL-1 and cholinergic signaling have anti-inflammatory activity (46, 47). Thus, our data portray the PSNS as the missing component linking osteo-immune physiology with both central IL-1 signaling and the autonomic nervous system.

Materials and Methods

Mice. Male mice were used throughout the study. All animal experiments were approved by the Hebrew University Committee of Animal Care and Use. Mice with homozygous transgenic overexpression of the secreted human IL-1ra in astrocytes within the central nervous system ($hIL1ra_{Ast}^{+/+}$) and mice deficient of the α_2nAChR subunit were reported previously (23, 29). The latter were kindly provided by Jim Boulter, Department of Psychiatry and Biobehavioral Sciences, University of California, Los Angeles, CA).

Retrograde Transneuronal Tracing of Skeletal Autonomic Innervation. Pseudorabies virus was injected into mouse or rat distal femoral metaphyses. Progression of immunoreactive pseudorabies virus was detected as described previously (24).

Heart Function. Heart rate was determined in WT and $hIL1raAst^{+/+}$ before and 30 min after intraperitoneal propranolol administration.

Immunohisto- and Cytochemistry. Decalcified femoral sections and culture dishes were reacted with anti-VAChT (Abcam), anti-α_2nAChR (Santa Cruz), and anti-β_2nAChR (Santa Cruz) antibodies. Sections were further processed using the SuperPicture Polymer detection Kit (Zymed Laboratories). Cultures were further reacted with anti-mouse Cy-3 conjugated antibody (Chemicon International), fluorescein-labeled phalloidin (Sigma-Aldrich) and DAPI (48) (Sigma-Aldrich).

mRNA Determination. Primer sets for semiquantitative and quantitative RT-PCR are reported in Table S3.

ACh Determination. ACh was extracted from freshly frozen distal femoral metaphyses. Its levels were measured using HPLC/MS/MS spectrometry (49).

In Vivo Skeletal Phenotyping. Histomorphometry and qualitative/quantitative μCT analyses were carried out as reported previously (23).

Bone Cell Cultures. Mouse bone marrow-derived ex vivo osteoclastogenic and primary newborn calvarial osteoblast cultures were as reported recently (50). Nicotinic receptor ligands were added together with macrophage colony-stimulating factor and RANKL. Pit formation was determined in cultures incubated on bovine dentin slices (30). Caspase-3 activity was measured using the CaspACE Assay System (Promega; catalog no. G7220) according to manufacturer instructions and expressed as release of *p*-nitroaniline per microgram of protein per hour.

Serum Markers of Bone Remodeling. Blood was collected retro-orbitally at the time of killing. Serum osteocalcin was determined using a two-site EIA kit (Biomedical Technologies). Mouse serum CTX was measured in the same specimens using an EIA kit (Wuhan EIAab Sciences).

Statistical Analysis. A *t* test was used when two samples were compared. Multiple means were compared by ANOVA. When significant differences were indicated by ANOVA, group means were compared using the Student Newman–Keuls test for pair-wise comparisons.

1. Rodan GA, Martin TJ (2000) Therapeutic approaches to bone diseases. *Science* 289: 1508–1514.
2. Elefteriou F, et al. (2005) Leptin regulation of bone resorption by the sympathetic nervous system and CART. *Nature* 434:514–520.
3. Katayama Y, et al. (2006) Signals from the sympathetic nervous system regulate hematopoietic stem cell egress from bone marrow. *Cell* 124:407–421.
4. Yirmiya R, et al. (2006) Depression induces bone loss through stimulation of the sympathetic nervous system. *Proc Natl Acad Sci USA* 103:16876–16881.
5. Tam J, et al. (2008) The cannabinoid CB1 receptor regulates bone formation by modulating adrenergic signaling. *FASEB J* 22:285–294.
6. Johnson RH, Spaulding JM (1974) Disorders of the autonomic nervous system. Chapter 3. The nervous control of the circulation and its investigation. *Contemp Neurol Ser* 11: 33–58.
7. Kawasaki A (1999) Physiology, assessment, and disorders of the pupil. *Curr Opin Ophthalmol* 10:394–400.
8. Kiba T (2004) Relationships between the autonomic nervous system and the pancreas including regulation of regeneration and apoptosis: Recent developments. *Pancreas* 29:e51–e58.
9. Manabe N, Tanaka T, Hata J, Kusunoki H, Haruma K (2009) Pathophysiology underlying irritable bowel syndrome—From the viewpoint of dysfunction of autonomic nervous system activity. *J Smooth Muscle Res* 45:15–23.
10. Young JA, Van Lennep EW (1977) Morphology and physiology of salivary myoepithelial cells. *Int Rev Physiol* 12:105–125.
11. Kandel ER, Schwartz JH, Jessell TM (2000) *Principles of Neural Science* (McGraw-Hill, New York), 4th Ed.
12. Loewi O (1921) Über humorale Übertragbarkeit der Herznervenwirkung [About humoral transmission of cardiac nerves effect]. *Pflugers Arch*, 189:239–242. German.
13. Nachmansohn D, John HM (1945) On the formation of acetylcholine in the nerve axon. *Science* 102:250–251.
14. Schäfer MK, Weihe E, Varoqui H, Eiden LE, Erickson JD (1994) Distribution of the vesicular acetylcholine transporter (VAChT) in the central and peripheral nervous systems of the rat. *J Mol Neurosci* 5:1–26.
15. Weihe E, Tao-Cheng JH, Schäfer MK, Erickson JD, Eiden LE (1996) Visualization of the vesicular acetylcholine transporter in cholinergic nerve terminals and its targeting to a specific population of small synaptic vesicles. *Proc Natl Acad Sci USA* 93:3547–3552.
16. Dani JA, Bertrand D (2007) Nicotinic acetylcholine receptors and nicotinic cholinergic mechanisms of the central nervous system. *Annu Rev Pharmacol Toxicol* 47:699–729.
17. Caulfield MP, Birdsall NJ (1998) International Union of Pharmacology. XVII. Classification of muscarinic acetylcholine receptors. *Pharmacol Rev* 50:279–290.
18. Taylor P, Radić Z (1994) The cholinesterases: From genes to proteins. *Annu Rev Pharmacol Toxicol* 34:281–320.
19. Shi Y, et al. (2010) Signaling through the M(3) muscarinic receptor favors bone mass accrual by decreasing sympathetic activity. *Cell Metab* 11:231–238.
20. En-Nosse M, et al. (2009) Expression of non-neuronal cholinergic system in osteoblast-like cells and its involvement in osteogenesis. *Cell Tissue Res* 338:203–215.
21. Krueger JM, et al. (1998) Sleep. A physiologic role for IL-1 beta and TNF-alpha. *Ann N Y Acad Sci* 856:148–159.
22. Avital A, et al. (2003) Impaired interleukin-1 signaling is associated with deficits in hippocampal memory processes and neural plasticity. *Hippocampus* 13:826–834.
23. Bajayo A, et al. (2005) Central IL-1 receptor signaling regulates bone growth and mass. *Proc Natl Acad Sci USA* 102:12956–12961.
24. Dénes A, et al. (2005) Central autonomic control of the bone marrow: Multisynaptic tract tracing by recombinant pseudorabies virus. *Neuroscience* 134:947–963.
25. Trotter RN, Stornetta RL, Guyenet PG, Roberts MR (2007) Transneuronal mapping of the CNS network controlling sympathetic outflow to the rat thymus. *Auton Neurosci* 131:9–20.
26. Cano G, Sved AF, Rinaman L, Rabin BS, Card JP (2001) Characterization of the central nervous system innervation of the rat spleen using viral transneuronal tracing. *J Comp Neurol* 439:1–18.
27. Tien D, Ohara PT, Larson AA, Jasmin L (2003) Vagal afferents are necessary for the establishment but not the maintenance of kainic acid-induced hyperalgesia in mice. *Pain* 102:39–49.
28. Marritt AM, et al. (2005) Nicotinic cholinergic receptors in the rat retina: Simple and mixed heteromeric subtypes. *Mol Pharmacol* 68:1656–1668.
29. Whiteaker P, et al. (2009) Pharmacological and immunochemical characterization of alpha2* nicotinic acetylcholine receptors (nAChRs) in mouse brain. *Acta Pharmacol Sin* 30:795–804.
30. Martin BR, Onaivi ES, Martin TJ (1989) What is the nature of mecamylamine's antagonism of the central effects of nicotine? *Biochem Pharmacol* 38:3391–3397.
31. Suda T, Jimi E, Nakamura I, Takahashi N (1997) Role of 1 alpha,25-dihydroxyvitamin D3 in osteoclast differentiation and function. *Methods Enzymol* 282:223–235.
32. Rothem DE, Rothem L, Soudry M, Dahan A, Eliakim R (2009) Nicotine modulates bone metabolism-associated gene expression in osteoblast cells. *J Bone Miner Metab* 27: 555–561.
33. Pedersen SE, Cohen JB (1990) d-Tubocurarine binding sites are located at alpha-gamma and alpha-delta subunit interfaces of the nicotinic acetylcholine receptor. *Proc Natl Acad Sci USA* 87:2785–2789.
34. Masson P (2011) Evolution of and perspectives on therapeutic approaches to nerve agent poisoning. *Toxicol Lett* 206:5–13.
35. Buisson B, Bertrand D (2002) Nicotine addiction: The possible role of functional up-regulation. *Trends Pharmacol Sci* 23:130–136.
36. Qin W, Bauman WA, Cardozo CP (2010) Evolving concepts in neurogenic osteoporosis. *Curr Osteoporos Rep* 8:212–218.
37. Romano SJ, Pugh PC, McIntosh JM, Berg DK (1997) Neuronal-type acetylcholine receptors and regulation of alpha 7 gene expression in vertebrate skeletal muscle. *J Neurobiol* 32:69–80.
38. Maletic V, Raison CL (2009) Neurobiology of depression, fibromyalgia and neuropathic pain. *Front Biosci* 14:5291–5338.
39. Liu PS, Chen YY, Feng CK, Lin YH, Yu TC (2011) Muscarinic acetylcholine receptors present in human osteoblast and bone tissue. *Eur J Pharmacol* 650:34–40.
40. Proskocil BJ, et al. (2004) Acetylcholine is an autocrine or paracrine hormone synthesized and secreted by airway bronchial epithelial cells. *Endocrinology* 145: 2498–2506.
41. Sato T, et al. (2010) Functional role of acetylcholine and the expression of cholinergic receptors and components in osteoblasts. *FEBS Lett* 584:817–824.
42. Yirmiya R, Bab I (2009) Major depression is a risk factor for low bone mineral density: A meta-analysis. *Biol Psychiatry* 66:423–432.
43. Pack AM, Reddy DS, Duncan S, Herzog A (2011) Neuroendocrinological aspects of epilepsy: Important issues and trends in future research. *Epilepsy Behav* 22:94–102.
44. Mineur YS, Picciotto MR (2010) Nicotine receptors and depression: Revisiting and revising the cholinergic hypothesis. *Trends Pharmacol Sci* 31:580–586.
45. Miwa JM, Freedman R, Lester HA (2011) Neural systems governed by nicotinic acetylcholine receptors: Emerging hypotheses. *Neuron* 70:20–33.
46. Sullivan GM, et al. (1997) Intracerebroventricular injection of interleukin-1 suppresses peripheral lymphocyte function in the primate. *Neuroimmunomodulation* 4:12–18.
47. Rosas-Ballina M, et al. (2008) Splenic nerve is required for cholinergic antiinflammatory pathway control of TNF in endotoxemia. *Proc Natl Acad Sci USA* 105: 11008–11013.
48. Colucci S, Colaianni G, Mori G, Grano M, Zallone A (2002) Human osteoclasts express oxytocin receptor. *Biochem Biophys Res Commun* 297:442–445.
49. Brown OM (1976) Cat heart acetylcholine: Structural proof and distribution. *Am J Physiol* 231:781–785.
50. Smoum R, et al. (2010) Oleoyl serine, an endogenous N-acyl amide, modulates bone remodeling and mass. *Proc Natl Acad Sci USA* 107:17710–17715.

Bajayo et al.